

# *In silico* fragment based design identifies subfamily B1 metallo- $\beta$ -lactamase inhibitors

Ricky Cain,<sup>[a]</sup> ‡ Jürgen Brem,<sup>[b]</sup> ‡ David Zollman,<sup>[b]</sup> Michael A. McDonough,<sup>[b]</sup> Rachel M. Johnson,<sup>[a]</sup> James Spencer,<sup>[c]</sup> Anne Makena,<sup>[b]</sup> Martine I. Abboud,<sup>[b]</sup> Samuel Cahill,<sup>[b]</sup> Sook Y. Lee,<sup>[b,d]</sup> Peter J. McHugh,<sup>[d]</sup> Christopher J. Schofield,<sup>[b]\*</sup> and Colin W. G. Fishwick <sup>[a]\*</sup>

<sup>[a]</sup> School of Chemistry, University of Leeds, Leeds, LS2 9JT, United Kingdom.

<sup>[b]</sup> Department of Chemistry, University of Oxford, 12 Mansfield Road, Oxford, OX1 3TA, United Kingdom.

<sup>[c]</sup> School of Cellular and Molecular Medicine, University of Bristol, Biomedical Sciences Building, Bristol, BS8 1TD, United Kingdom.

<sup>[d]</sup> Department of Oncology, Weatherall Institute of Molecular Medicine, University of Oxford, John Radcliffe Hospital, Oxford, United Kingdom.

E-mail: [christopher.schofield@chem.ox.ac.uk](mailto:christopher.schofield@chem.ox.ac.uk) and [c.w.g.fishwick@leeds.ac.uk](mailto:c.w.g.fishwick@leeds.ac.uk)

## ABSTRACT

Zinc ion dependent  $\beta$ -lactamases (MBLs) catalyze the hydrolysis of almost all  $\beta$ -lactam antibiotics and resist the action of clinically available  $\beta$ -lactamase inhibitors. We report how application of *in silico* fragment-based molecular design employing thiol-mediated metal

anchorage leads to potent MBL inhibitors. The new inhibitors manifest potent inhibition of clinically important B1 subfamily MBLs, including the widespread NDM-1, IMP-1 and VIM-2 enzymes; with lower potency, some of them also inhibit clinically relevant Class A and D serine- $\beta$ -lactamases. The inhibitors show selectivity for bacterial MBL enzymes compared to human MBL fold nucleases. Co-crystallization of one inhibitor, which shows potentiation of meropenem activity against MBL-expressing *Enterobacteriaceae*, with VIM-2 reveals an unexpected binding mode, involving interactions with residues from conserved active site bordering loops.

## INTRODUCTION

$\beta$ -Lactam containing inhibitors remain the single most important antibacterials.<sup>1, 2</sup>  $\beta$ -Lactams inhibit transpeptidases (or penicillin-binding proteins, PBPs) involved in cell wall biosynthesis by reacting with a catalytically crucial nucleophilic serine residue. Bacteria have developed multiple resistance mechanisms to  $\beta$ -lactams, most importantly by  $\beta$ -lactamase catalysed hydrolysis. There are four classes of  $\beta$ -lactamases:<sup>3</sup> classes A, C, and D are serine- $\beta$ -lactamases (SBLs), which are mechanistically related to the PBPs; class B are metallo- $\beta$ -lactamases (MBLs), employing (a) zinc ion(s) in catalysis.

Co-administration of a  $\beta$ -lactam antibacterial with a class A  $\beta$ -lactamase inhibitor (clavulanic acid,<sup>4</sup> tazobactam,<sup>5</sup> sulbactam) has successfully overcome some SBL-mediated resistance. Avibactam,<sup>6</sup> a non  $\beta$ -lactam broader spectrum inhibitor of class A, C, and some class D SBLs, has recently been introduced into the clinic.<sup>7</sup> As yet there are, however, no reports of clinically useful class B MBL inhibitors (Figure 1a).<sup>8-11</sup> MBLs are a concern because they catalyze hydrolysis of almost all  $\beta$ -lactam antibacterials, including the carbapenems, which are commonly used for treatment of severe and highly resistant infections. MBLs are divided into the B1, B2,

and B3 subclasses based on metal site occupancy and sequence similarity.<sup>12-14</sup> Subclass B1 MBLs, which employ two zinc ions (Zn-1/Zn-2) are the most clinically relevant and include the New Delhi metallo- $\beta$ -lactamase (NDM-1), Verona integron-encoded MBL (VIM), and Imipenemase (IMP) types of B1 MBLs.

Combating increasing resistance mediated by MBLs requires the identification of either novel antibacterials or MBL resistant  $\beta$ -lactams (both likely substantial undertakings), or developing an MBL inhibitor for co-administration with an existing  $\beta$ -lactam. Here we report how the application of *in silico* fragment-based<sup>15, 16</sup> molecular design led to identification of potent inhibitors of clinically relevant MBLs, some of which have (lower) activity against certain SBLs. The *in silico* studies employed a structure-guided approach in which fragments were anchored to the di zinc ion centre *via* a thiol and then optimised for binding *via* hydrophilic and electrostatic interactions. Whilst such metal anchorage (or 'support ligand') based approach has been applied in dynamic combinatorial based identification<sup>17</sup> of ligands to MBLs, to our knowledge this is the first application of an *in silico* fragment-based approach for production of specific MBL inhibitors.

## RESULTS AND DISCUSSION

### ***De Novo* Ligand Design**

The *de novo* molecular design program SPROUT<sup>15, 16</sup> generates potential ligands *via* docking of fragments into targeted regions; subsequent user-directed assembly using template spacers to link these fragments together yields synthetically tractable scaffolds (Figure 1b). Analysis of an crystal structure of NDM-1 structure complexed with hydrolysed ampicillin (PDB code 3Q6X)<sup>14</sup> using SPROUT<sup>16</sup> identified active site regions for targeting with *in silico*-generated fragments,

i.e. the regions proximal to: the Lys224 side chain, the Zn-2 metal ion, the nucleophilic hydroxide / water that “bridges” the two zinc ions, and a conserved tryptophan (Trp87) that makes hydrophobic interactions with the aromatic ampicillin C6 side chain<sup>18</sup> (Figure 1c). Importantly, while details differ between individual MBLs, these features are predicted to be crucial for  $\beta$ -lactam binding by most, if not all, B1 MBLs.<sup>10</sup> This design approach led to the identification of a simple benzyl thiol **1** (Figure 1) as a potential NDM-1 substrate-competitive inhibitor. A detailed, step-by step description of the *in silico* fragment based design *de novo* design is given in the SPROUT utilizing design sections (Supporting Information).

The *in silico* predicted interactions of **1** with NDM-1 include interaction between its carboxylate and the Lys224 side chain and the Zn-2 ion; anchoring of its thiol with both Zn-1 and Zn-2; and between the aryl ring of **1** with Trp87, via  $\pi$ -stacking interactions (Figure 2a). Compound **1** was synthesized using Suzuki coupling (67%)<sup>19</sup> of 5-bromophthalide and phenyl boronic acid to give a lactone which was ring-opened using Me<sub>3</sub>SiI to give the corresponding iodide (62%). Iodide displacement using thiourea, followed by hydrolysis gave **1** (81%; see Methods and Supporting Information for details).

Using a fluorogenic MBL assay<sup>20</sup> **1** was then evaluated for inhibition of recombinant forms of NDM-1, IMP-1, and VIM-2. Inhibition studies with **1** and subsequent compounds were conducted in the presence of 0.01% Triton X-100 to reduce the potential of identifying protein aggregating compounds<sup>21-23</sup>. The results (Table 1) reveal **1** to be an inhibitor with sub-micromolar IC<sub>50</sub> values for all three of the tested B1 MBLs, with IC<sub>50</sub> values 232 – 234 nM; these values compare favourably with the thiol-MBL inhibitors such as *L*-captopril for which IC<sub>50</sub> values against B1 MBLs are in the micromolar range.<sup>10</sup>

## Crystallographic studies

To investigate the binding of **1** with B1 MBLs, a structure of it complexed with VIM-2 was obtained by co-crystallization (1.74 Å resolution; space group  $C2_1$ ; see Supporting Information, Figure S1 and Table S1). As predicted by the design studies, analysis of the crystal structure confirms that the thiol of **1** acts as a metal binding ligand that displaces the proposed ‘hydrolytic’ hydroxide ion bridging the two metal ions (Figure 2b). The crystallographically observed conformation of the biphenyl unit in VIM-2 was not, however, as predicted for NDM-1 (Figure 1 and Figure 2a); unexpectedly, the aryl carboxylate of **1** is positioned to interact with Trp87 of VIM-2 and, *via* a water molecule, with Asp119, rather than with Arg228 (analogous to Lys 224 in NDM-1) (Figure 2b). In the VIM-2 structure, **1** presents two binding faces, as also present in the predicted  $\beta$ -lactam substrate, and observed hydrolysed  $\beta$ -lactam, binding modes.<sup>10</sup> One face is hydrophobic and interacts with the substantially hydrophobic L3 loop, via apparent  $\pi$ -stacking of the aryl ring of **1** with Tyr67 and interactions with Trp87 (Figure 2b). The other binding face of **1** involves electrostatic and hydrogen bonding interactions with residues from L10 loop, apparent interaction between the Arg228 guanidino group and the phenyl ring of **1** (3.8 Å), and potential interaction between one of the carboxylate oxygen’s of **1** with the side chain amide of Asn233 (3.6 Å). The difference in the predicted NDM-1 binding mode for **1** versus the crystallographically observed binding mode of **1** with VIM-2 may, in part, reflect the removal of water molecules from the NDM-1 structure prior to application of SPROUT to simplify the calculations, as well as active site differences between the two enzymes<sup>15, 16</sup> (see Supporting Information).

## Structure Activity Relationship Studies

Following the encouraging levels of inhibition observed with **1**, we conducted structure activity relationship (SAR) studies. Modification of the terminal phenyl ring of **1** (Table 1) revealed no clear trend in potency when changing the electron density or steric bulk, via incorporation of bromine (**17**) or five-membered ring substituents (**15** and **16**), implying that the  $\pi$ -stacking interaction with Tyr67 is not crucial for affinity. Similarly, positioning substituents in the *ortho*-position of the phenyl ring (**4**, **9** and **10**), to investigate whether changes to the dihedral angle between the aryl rings might affect affinity, did not yield substantial changes in potency. The importance of the spatial arrangement of functional groups was investigated via **19** (Supporting Information, Figure S5) in which the methylene linking the thiol to the phenyl ring is switched to link the carboxylic acid. The thiolactone **18**, (Supporting Information, Figure S4) was synthesised to test whether it undergoes hydrolysis to **1** (Supporting Information, Table S2). Neither **18** nor **19** manifested significant activity against VIM-2 ( $IC_{50} > 100 \mu M$ ) showing that the arrangement of the functional groups is important and indicating that the thiolactone **18** does not appear to be an efficient substrate for VIM-2.

**2-17** were evaluated for inhibition against NDM-1 and IMP-1 (Table 1 and Supporting Information, Table S2); selected compounds (**4-8**) were screened against the model MBL BcII and the 'hybrid' B1/B2 like MBL SPM-1.<sup>24</sup> The results reveal **4-8** to be active against BcII and SPM-1, with  $IC_{50}$  values  $0.78 - 7.8 \mu M$  (Supporting Information, Table S3). Moreover, except for **11**, all compounds manifested sub-micromolar  $IC_{50}$  values against IMP-1 with several compounds showing sub-micromolar activity against NDM-1 (**5**, **6**, **7**, **8** and **13**). Binding of selected inhibitors to VIM-2 and NDM-1 was investigated by NMR.<sup>25, 26</sup> The  $^1H$  CPMG NMR results validated<sup>25</sup> binding of **1** and **9** to VIM-2 and  $^{19}F$  NMR<sup>26</sup> was used to validate binding to

NDM-1 (Supporting Information, Figure S7). Consistent with the inhibition data, the NMR analyses show that **1** and **9** bind with  $K_D$  values  $< 1 \mu\text{M}$  to VIM-2 and **9** out competes **11** for binding to NDM-1 (Supporting Information, Figure S8).

In the initial assessment of our inhibitors as hits we screened **4** and **9** against the SBL AmpC<sup>21</sup>; **4** and **9** showed activity against AmpC both in the presence and absence of Triton X-100 (Supplementary Information, Table S4). We then screened **1**, **7**, **8** and **9** against TEM-1, AmpC, and OXA-10, which are representatives of Class A, C, and D SBLs, respectively (Supporting Information, Table S4). Interestingly, **8** and **9** inhibited TEM-1 and **9** inhibited OXA-10 ( $\text{IC}_{50}$ s 32.8, 5.5 and 37.3  $\mu\text{M}$ , respectively, Supporting Information, Table S4). Although we have been unable to obtain structures of these compounds complexed with SBLs, these results show some of the inhibitors could interact with both SBLs and MBLs via related binding modes as shown in Figure 2); indeed, our predicted binding mode of **1** to TEM-1 and OXA-10 is similar to that observed crystallographically for a recently identified biphenyl carboxylic acid obtained through a surface plasmon resonance (SPR) based screen for inhibitors of the OXA-48 SBL<sup>27</sup>. However, the unexpected crystallographically observed binding mode of **1** to VIM-2 (Figure 2) means caution should be exercised in predicting the SBL binding modes of our compounds.

### Selectivity screening

Clinically relevant MBL inhibitors should show selectivity towards the bacterial MBLs over human metallo-enzymes, including human MBL-fold enzymes.<sup>28</sup> We tested **1**, **5**, **13** and **17** against two human MBL fold enzymes involved in DNA repair, DNA cross-link repair enzymes 1A and B (DCLRE1A and DCLRE1B). DCLRE1A was only weakly inhibited by **1** ( $\text{IC}_{50}$   $247 \pm 154 \mu\text{M}$ ) and DCLRE1B was inhibited by **1**, **5** and **17** ( $\text{IC}_{50}$ s  $149 \pm 27$ ,  $268 \pm 112$  and  $185 \pm 50$

μM, respectively), implying, at least partial, selectivity of the compounds towards the bacterial MBLs. Compound **1** showed good aqueous solubility and underwent moderate metabolism in human liver microsomes (see Supporting Information).

### Antibacterial Activity

Compounds **1** and **11-17** were screened in minimal inhibitory concentration (MIC) antimicrobial assays, in co-administration studies with the clinically important carbapenem meropenem, using MBL producing strains of *E. coli* and *K. pneumoniae* (species where NDM-1 production is a growing clinical problem).<sup>29</sup> Tests in the absence of inhibitors manifested meropenem MICs against MBL-producing bacteria of >128 μg/ml, and that when tested alone **1** has no antibacterial activity within limits of detection (Table 2). Encouragingly, at 100 μg/ml all tested compounds, apart from **11**, reduced the MIC of meropenem against NDM-1-producing strains. Compound **16** showed the strongest activity, reducing the meropenem MIC to 8 μg/ml against *K. pneumoniae*.

### CONCLUSIONS

Overall, the results reveal how computer aided design can help generate broad spectrum MBL inhibitors active against three types of clinically important B1 MBLs, as well as some SBLs. The inhibitors can reduce MICs of meropenem against MBL-producing bacteria, indicating they are suitable for further development. Unlike some reported MBL inhibitors,<sup>30</sup> our compounds bind directly to the MBL active sites, i.e. do not function by removing the zinc ions, as shown by NMR and crystallographic analyses.<sup>31</sup> While utilizing its thiol to bind the MBL active site by intercalating between the two B1 MBL subclass zinc ions has precedent,<sup>8</sup> the

crystallographically observed mode of binding **1** with VIM-2 (Figure 1), has not been previously observed. The difference between the crystallographically observed binding mode for **1** with VIM-2 and that predicted for NDM-1 (Figure 2) indicates how differences in closely related metallo-enzymes can apparently enable different binding modes of the same inhibitors, even when they are anchored in the same manner, i.e. to the two active site zinc ions of the B1 MBLs. It may also reflect of limitations in our current computational methodology, including with an inability to deal with solvation.

The observation of activity for the designed compounds against several different types of clinically relevant B1 MBLs is notable (Table 1) because inhibition of a spectrum of MBLs is a likely prerequisite for clinical application of an MBL inhibitor. Although the compounds described here are unlikely to be of direct clinical utility, the work suggests that computational chemistry can have an important role in designing inhibitors that are active for use against both current and future predicted antibacterial resistance mediated by  $\beta$ -lactamases. The need for an ability to rapidly optimise against emerging resistance is highlighted by the identifications of the multiple class B1 MBL variants already identified.<sup>12</sup> Our approach may have utility in efficiently identifying other inhibitor chemotypes involving alternative metal-coordinating moieties, as well as inhibitors not relying on metal coordination.

## EXPERIMENTAL SECTION

The Supporting Information contains a complete general experimental section, including all procedures and equipment used. Chemicals were from commonly used suppliers (Aldrich, Acros, and Alfa Aesar) and used without purification. The purity of compounds submitted for screening

was  $\geq 95\%$  as determined by UV analysis of liquid chromatography (HPLC) chromatograms at 254 nm.

#### **General procedure for the Suzuki cross coupling reaction**

The boronic acid (1.1 equiv.) was added to a stirred solution of 5-bromophthalide (1.0 equiv.), potassium carbonate (1.0 equiv.) and tetrakis(triphenylphosphine) palladium (0) (0.05 equiv.) in THF (4 mL) and water (2 mL). The reaction mixture was heated at reflux for 12 h, then filtered through Celite®, and concentrated *in vacuo*. The residue was diluted with water (20 mL), then extracted using dichloromethane (3  $\times$  20 mL). The combined organic extracts were dried (MgSO<sub>4</sub>) and concentrated *in vacuo* to give a pale-yellow solid, which was purified using flash column chromatography to afford the coupled product.

#### **General procedure for lactone opening with iodotrimethylsilane forming the iodides**

The benzofuranone (1.0 equiv.) was dissolved in dichloromethane (4.5 mL); TMSI (1.5 equiv.) was then added and the reaction was refluxed under nitrogen for 3 h. After this time, the mixture was cooled to room temperature and quenched with water (3 mL). The precipitate was isolated by filtration washing with water (2  $\times$  10 mL) to give the desired iodide product as an off-white solid, which was used without further purification.

#### **General procedure for introduction of the thiol<sup>32</sup>**

A mixture of thiourea (1.1 equiv.) in THF (3 mL) was heated to reflux. To this mixture was added the iodide product of the previous procedure (1.0 equiv.). The reaction mixture was heated at reflux for 16 h under nitrogen. The reaction mixture was then cooled to room temperature and concentrated *in vacuo*. The residue was re-suspended in 2M aqueous NaOH (5 mL) and the solution refluxed for 3 h. The reaction mixture then acidified with 2M aqueous HCl to ~pH2. The colorless precipitate was isolated by filtration.

## Representative synthesis: for compound 1

### Synthesis of 5-phenyl-1,3-dihydro-2-benzofuranone

Phenyl boronic acid (0.32 g, 2.58 mmol, 1.1 equiv.) was added to a stirred solution of 5-bromophthalide (0.50 g, 2.35 mmol, 1.0 equiv.), potassium carbonate (0.33 g, 2.35 mmol, 1.0 equiv.) and tetrakis(triphenylphosphine) palladium (0) (0.14 g, 0.12 mmol, 0.05 equiv.) in THF (4 mL) and water (2 mL). The reaction mixture was heated to reflux for 12 h, then filtered through Celite®, and concentrated *in vacuo*. The residue was diluted with water (20 mL) and extracted using dichloromethane (3 × 20 mL). The combined organic extracts were dried (MgSO<sub>4</sub>), then concentrated *in vacuo* to give a pale-yellow solid, which was purified by flash column chromatography to afford the desired product as a cream colored solid, which was used without further purification. (0.33 g, 1.58 mmol, 67%) m.p.: 124.4-125.8 °C; R<sub>f</sub>: 0.5 (2:1 petrol-EtOAc); δH (300 MHz, CDCl<sub>3</sub>): 7.98 (1H, d, J 7.6, 3-H), 7.75 (1H, d, J 7.6, 4-H), 7.68 (1H, s, 6-H), 7.62 (2H, d, J 7.1, 2'-H and 6'-H), 7.47 (2H, app. t, J 7.1, 3'-H and 5'-H) 7.45 (1H, t, J 7.1, 4'-H), 5.38 (2H, s, CH<sub>2</sub>O); δC (75 MHz, CDCl<sub>3</sub>): 147.5 (C=O), 147.3 (C1), 139.6 (C3), 129.1 (C3'' and C5'), 128.6 (C2), 128.5 (C5), 127.5 (C2' and C6') 126.1 (C4'), 124.5 (C1'), 120.6 (C6), 69.9 (CH<sub>2</sub>O); ν<sub>max</sub>/ cm<sup>-1</sup> (solid): 3473, 3070, 2924, 1747, 1615, 1452; HPLC: Tr= 3.00 (100% rel. area); m/z (ES): (Found: MNa<sup>+</sup>, 233.0573. C<sub>14</sub>H<sub>10</sub>O<sub>2</sub> requires MNa, 223.0570).

### Synthesis of 2-iodomethyl-4-phenyl-benzoic acid

5-Phenyl-1,3-dihydro-2-benzofuranone (0.20 g, 0.95 mmol, 1.0 equiv.) was dissolved in dichloromethane (4.5 mL). TMSI (0.20 mL, 1.43 mmol, 1.5 equiv.) was added and the reaction was refluxed under nitrogen for 3 h. The mixture was then cooled to room temperature and quenched with water (3 mL). The precipitate was isolated by filtration, washing with water (2 ×

10 mL) to give the desired product as a pale brown solid, which was used without further purification. (0.20 g, 0.59 mmol, 62%) m.p.: 81.3-82.4 °C;  $R_f$ : 0.75 (CHCl<sub>3</sub>);  $\delta H$  (300MHz, DMSO-d<sub>6</sub>): 7.94 (1H, d, J 8.3, 6-H), 7.88 (1h, d, J 1.8, 3-H), 7.73 (2H, d, J 7.3, 6'-H and 2'-H), 7.68 (1H, dd, J 8.3 and 1.8, 5-H), 7.51 (2H, app. t, J 7.3, 5'-H and 3'-H), 7.44 (1H, t, J 7.3, 4'-H), 5.09 (2H, s, CH<sub>2</sub>);  $\nu_{max}$ / cm<sup>-1</sup> (solid): 2806, 2630, 1750, 1603, 1257, 909; m/z (ES): (Found: [M+2Na-H]<sup>+</sup>, 382.9516. C<sub>14</sub>H<sub>11</sub>IO<sub>2</sub> requires [M+2Na-H], 382.9515).

### Synthesis of 4-phenyl-2-sulfonylmethylbenzoic acid (1)

A mixture of thiourea (0.16 g, 2.11 mmol, 1.1 equiv.) and 2-Iodomethyl-4-phenyl-benzoic acid (0.65 g, 1.92 mmol, 1.0 equiv.) in THF was heated at reflux for 16 h under an atmosphere of nitrogen, then cooled to room temperature. The mixture was then concentrated *in vacuo*, then re-suspended in 2M aqueous NaOH (5 mL) and refluxed for 3 h. The resultant mixture then acidified with 2M aqueous HCl to ~pH2. The pale yellow microcrystals were isolated by filtration. C<sub>14</sub>H<sub>10</sub>Cl<sub>2</sub>O<sub>2</sub>S requires [M-H], 310.9706). (0.25 g, 1.01 mmol, 53%). m.p.: 168.2-169.9 °C;  $R_f$ : 0.20 (19:1 DCM-MeOH);  $\delta H$  (300 MHz, DMSO-d<sub>6</sub>): 7.95 (1H, d, J 8.2, 6-H), 7.77 (1H, d, J 2.0, 3-H), 7.73 (2H, d, J 7.4, 6'-H and 2'-H), 7.65 (1H, dd, J 8.2 and 2.0, 5-H), 7.52 (2H, app. t, J 7.4, 5'-H and 3'-H), 7.44 (1H, t, J 7.4, 4'-H), 4.13 (2H, d, J 8.5, CH<sub>2</sub>), 2.87 (1H, t, J 8.5, SH);  $\delta C$  (75 MHz, DMSO-d<sub>6</sub>): 168.0 (C=O), 144.3 (C<sub>4</sub>), 143.6 (C<sub>1'</sub>), 138.7 (C<sub>2</sub>), 131.5 (C<sub>6</sub>), 129.0 (C<sub>5'</sub> and C<sub>3'</sub>), 128.9 (C<sub>4'</sub>), 128.2 (C<sub>5</sub>), 127.8 (C<sub>1</sub>), 126.9 (C<sub>6'</sub> and C<sub>2'</sub>), 124.9 (C<sub>3</sub>), 26.4 (CH<sub>2</sub>);  $\nu_{max}$ / cm<sup>-1</sup> (solid): 2976, 1681, 1350, 1278, 756; HPLC: Tr= 2.88 (95% rel. area); m/z (ES): (Found: [M-H]<sup>-</sup>, 243.0477 C<sub>14</sub>H<sub>12</sub>O<sub>2</sub>S requires [M-H], 243.0485).

## ASSOCIATED CONTENT

### Supporting Information.

The following files are available free of charge.

Experimental procedures, characterization of intermediates and target compounds, description of protein production and purification, biological assays and determination of IC<sub>50</sub> values. (PDF)

### Accession Codes

PDB ID code: VIM-2 with bound **1** is 5K48. Authors will release the atomic coordinates and experimental data upon article publication.

## AUTHOR INFORMATION

### Corresponding Authors

\*Christopher J. Schofield Phone: +44 (0) 1865 275625 E-mail: [christopher.schofield@chem.ox.ac.uk](mailto:christopher.schofield@chem.ox.ac.uk) and Colin W. G. Fishwick Phone: +44 (0) 1133 436510 E-mail: [c.w.g.fishwick@leeds.ac.uk](mailto:c.w.g.fishwick@leeds.ac.uk)

### Author Contributions

<sup>‡</sup>R.C. and J.B. contributed equally to this work.

### Notes

The authors declare no competing financial interests.

### Acknowledgements

We thank the Medical Research Council (MRC)/Canadian Grant G1100135 (RC, JS, CWGF, JB and CJS), the Wellcome Trust, and the Biotechnology and Biological Research Council for funding (BBSRC). This work was supported by Cancer Research UK (CR-UK) grant number C5255/A18085, through the Cancer Research UK Oxford Centre (JB).

#### ABBREVIATIONS USED

MBL, metallo- $\beta$ -lactamase; SBL, serine- $\beta$ -lactamase; TMSI, iodotrimethylsilane.

## References

1. Hamad, B. The antibiotics market. *Nat. Rev. Drug Discov.* **2010**, *9*, 675-676.
2. Molstad, S.; Lundborg, C. S.; Karlsson, A. K.; Cars, O. Antibiotic prescription rates vary markedly between 13 European countries. *Scand. J. Infect. Dis.* **2002**, *34*, 366-371.
3. Ambler, R. P. The structure of  $\beta$ -lactamases. *Phil. Trans. R. Soc. B* **1980**, *289*, 321-331.
4. Arulanantham, H.; Kershaw, N. J.; Hewitson, K. S.; Hughes, C. E.; Thirkettle, J. E.; Schofield, C. J. ORF17 from the clavulanic acid biosynthesis gene cluster catalyzes the ATP-dependent formation of N-glycyl-clavaminic acid. *J. Biol. Chem.* **2006**, *281*, 279-287.
5. Yang, Y.; Rasmussen, B. A.; Shlaes, D. M. Class A  $\beta$ -lactamases-enzyme-inhibitor interactions and resistance. *Pharmacol. Ther.* **1999**, *83*, 141-151.
6. Li, H.; Estabrook, M.; Jacoby, G. A.; Nichols, W. W.; Testa, R. T.; Bush, K. In vitro susceptibility of characterized  $\beta$ -lactamase-producing strains tested with avibactam combinations. *Antimicrob. Agents. Chemother.* **2015**, *59*, 1789-1793.
7. Stone, G. G.; Bradford, P. A.; Newell, P.; Wardman, A. In vitro activity of ceftazidime-avibactam against isolates in a phase 3 open-label clinical trial for complicated intra-abdominal and urinary tract infections caused by ceftazidime-nonsusceptible gram-negative pathogens. *Antimicrob. Agents. Chemother.* **2017**, *61*, e01820-16.
8. Faridoon; UI Islam, N. An update on the status of potent inhibitors of metallo- $\beta$ -lactamases. *Sci. Pharm.* **2013**, *81*, 309-327.
9. Cahill, S. T.; Cain, R.; Wang, D. Y.; Lohans, C. T.; Wareham, D. W.; Oswin, H. P.; Mohammed, J.; Spencer, J.; Fishwick, C. W.; McDonough, M. A.; Schofield, C. J.; Brem, J.

Cyclic boronates inhibit all classes of  $\beta$ -lactamases. *Antimicrob. Agents. Chemother.* **2017**, *61*, e02260-16.

10. Brem, J.; van Berkel, S. S.; Zollman, D.; Lee, S. Y.; Gileadi, O.; McHugh, P. J.; Walsh, T. R.; McDonough, M. A.; Schofield, C. J. Structural basis of metallo- $\beta$ -lactamase inhibition by captopril stereoisomers. *Antimicrob. Agents. Chemother.* **2015**, *60*, 142-150

11. Brem, J.; van Berkel, S. S.; Aik, W.; Rydzik, A. M.; Avison, M. B.; Pettinati, I.; Umland, K. D.; Kawamura, A.; Spencer, J.; Claridge, T. D.; McDonough, M. A.; Schofield, C. J. Rhodanine hydrolysis leads to potent thioenolate mediated metallo- $\beta$ -lactamase inhibition. *Nat. Chem.* **2014**, *6*, 1084-1090.

12. Cornaglia, G.; Giamarellou, H.; Rossolini, G. M. Metallo- $\beta$ -lactamases: a last frontier for  $\beta$ -lactams? *Lancet Infect. Dis.* **2011**, *11*, 381-393.

13. Bebrone, C.; Delbruck, H.; Kupper, M. B.; Schlomer, P.; Willmann, C.; Frere, J. M.; Fischer, R.; Galleni, M.; Hoffmann, K. M. The structure of the dizinc subclass B2 metallo- $\beta$ -lactamase CphA reveals that the second inhibitory zinc ion binds in the histidine site. *Antimicrob. Agents. Chemother.* **2009**, *53*, 4464-4471.

14. Zhang, H.; Hao, Q. Crystal structure of NDM-1 reveals a common  $\beta$ -lactam hydrolysis mechanism. *FASEB J.* **2011**, *25*, 2574-2582.

15. Gillet, V.; Johnson, A. P.; Mata, P.; Sike, S.; Williams, P. SPROUT: a program for structure generation. *J. Comput. Aided. Mol. Des.* **1993**, *7*, 127-153.

16. Gillet, V. J.; Newell, W.; Mata, P.; Myatt, G.; Sike, S.; Zsoldos, Z.; Johnson, A. P. SPROUT: recent developments in the de novo design of molecules. *J. Chem. Inf. Comput. Sci.* **1994**, *34*, 207-217.

17. Demetriades, M.; Leung, I. K.; Chowdhury, R.; Chan, M. C.; McDonough, M. A.; Yeoh, K. K.; Tian, Y. M.; Claridge, T. D.; Ratcliffe, P. J.; Woon, E. C.; Schofield, C. J. Dynamic combinatorial chemistry employing boronic acids/boronate esters leads to potent oxygenase inhibitors. *Angew. Chem. Int. Ed. Engl.* **2012**, *51*, 6672-6675.
18. Brem, J.; Cain, R.; Cahill, S.; McDonough, M. A.; Clifton, I. J.; Jimenez-Castellanos, J. C.; Avison, M. B.; Spencer, J.; Fishwick, C. W.; Schofield, C. J. Structural basis of metallo- $\beta$ -lactamase, serine- $\beta$ -lactamase and penicillin-binding protein inhibition by cyclic boronates. *Nat. Commun.* **2016**, *7*, 12406.
19. Miyaura, N.; Yamada, K.; Suzuki, A. A new stereospecific cross-coupling by the palladium-catalyzed reaction of 1-alkenylboranes with 1-alkenyl or 1-alkynyl halides. *Tetrahedron Lett.* **1979**, *20*, 3437-3440.
20. van Berkel, S. S.; Brem, J.; Rydzik, A. M.; Salimraj, R.; Cain, R.; Verma, A.; Owens, R. J.; Fishwick, C. W.; Spencer, J.; Schofield, C. J. Assay platform for clinically relevant metallo- $\beta$ -lactamases. *J. Med. Chem.* **2013**, *56*, 6945-6953.
21. Irwin, J. J.; Duan, D.; Torosyan, H.; Doak, A. K.; Ziebart, K. T.; Sterling, T.; Tumanian, G.; Shoichet, B. K. An aggregation advisor for ligand discovery. *J. Med. Chem.* **2015**, *58*, 7076-7087.
22. Shoichet, B. K. Interpreting steep dose-response curves in early inhibitor discovery. *J. Med. Chem.* **2006**, *49*, 7274-7277.
23. Feng, B. Y.; Simeonov, A.; Jadhav, A.; Babaoglu, K.; Inglese, J.; Shoichet, B. K.; Austin, C. P. A high-throughput screen for aggregation-based inhibition in a large compound library. *J. Med. Chem.* **2007**, *50*, 2385-2390.

24. Brem, J.; Struwe, W. B.; Rydzik, A. M.; Tarhonskaya, H.; Pfeffer, I.; Flashman, E.; van Berkel, S. S.; Spencer, J.; Claridge, T. D.; McDonough, M. A.; Benesch, J. L.; Schofield, C. J. Studying the active-site loop movement of the Sao Paulo metallo- $\beta$ -lactamase-1. *Chem. Sci.* **2015**, *6*, 956-963.
25. Mashalidis, E. H.; Sledz, P.; Lang, S.; Abell, C. A three-stage biophysical screening cascade for fragment-based drug discovery. *Nat. Protoc.* **2013**, *8*, 2309-2324.
26. Gee, C. T.; Arntson, K. E.; Urick, A. K.; Mishra, N. K.; Hawk, L. M.; Wisniewski, A. J.; Pomerantz, W. C. Protein-observed  $^{19}\text{F}$ -NMR for fragment screening, affinity quantification and druggability assessment. *Nat. Protoc.* **2016**, *11*, 1414-1427.
27. Lund, B. A.; Christopeit, T.; Guttormsen, Y.; Bayer, A.; Leiros, H. K. Screening and design of inhibitor scaffolds for the antibiotic resistance oxacillinase-48 (OXA-48) through surface plasmon resonance screening. *J. Med. Chem.* **2016**, *59*, 5542-5554.
28. Pettinati, I.; Brem, J.; McDonough, M. A.; Schofield, C. J. Crystal structure of human persulfide dioxygenase: structural basis of ethylmalonic encephalopathy. *Hum. Mol. Genet.* **2015**, *24*, 2458-2469.
29. Khan, A. U.; Maryam, L.; Zarrilli, R. Structure, genetics and worldwide spread of New Delhi metallo- $\beta$ -lactamase (NDM): a threat to public health. *BMC Microbiol.* **2017**, *17*, 101.
30. McGeary, R. P.; Tan, D. T.; Schenk, G. Progress toward inhibitors of metallo- $\beta$ -lactamases. *Future Med. Chem.* **2017**, *9*, 673-691.
31. Li, G. B.; Abboud, M. I.; Brem, J.; Someya, H.; Lohans, C. T.; Yang, S. Y.; Spencer, J.; Wareham, D. W.; McDonough, M. A.; Schofield, C. J. NMR-filtered virtual screening leads to non-metal chelating metallo- $\beta$ -lactamase inhibitors. *Chem. Sci.* **2017**, *8*, 928-937.

32. Cossar, B. C.; Fournier, J. O.; Fields, D. L.; Reynolds, D. D. Preparation of Thiols. *J. Org. Chem.* **1962**, 27, 93-95.

**Figure 1.** Design of broad spectrum MBL inhibitors. A) Known MBL binders (inhibitors) and compound **1**.<sup>8-11</sup> B) Key elements used in the SPROUT computational design process leading to the identification of putative broad spectrum MBL inhibitors. C) Outline mechanism for SBLs and MBLs as shown for a penicillin substrate.

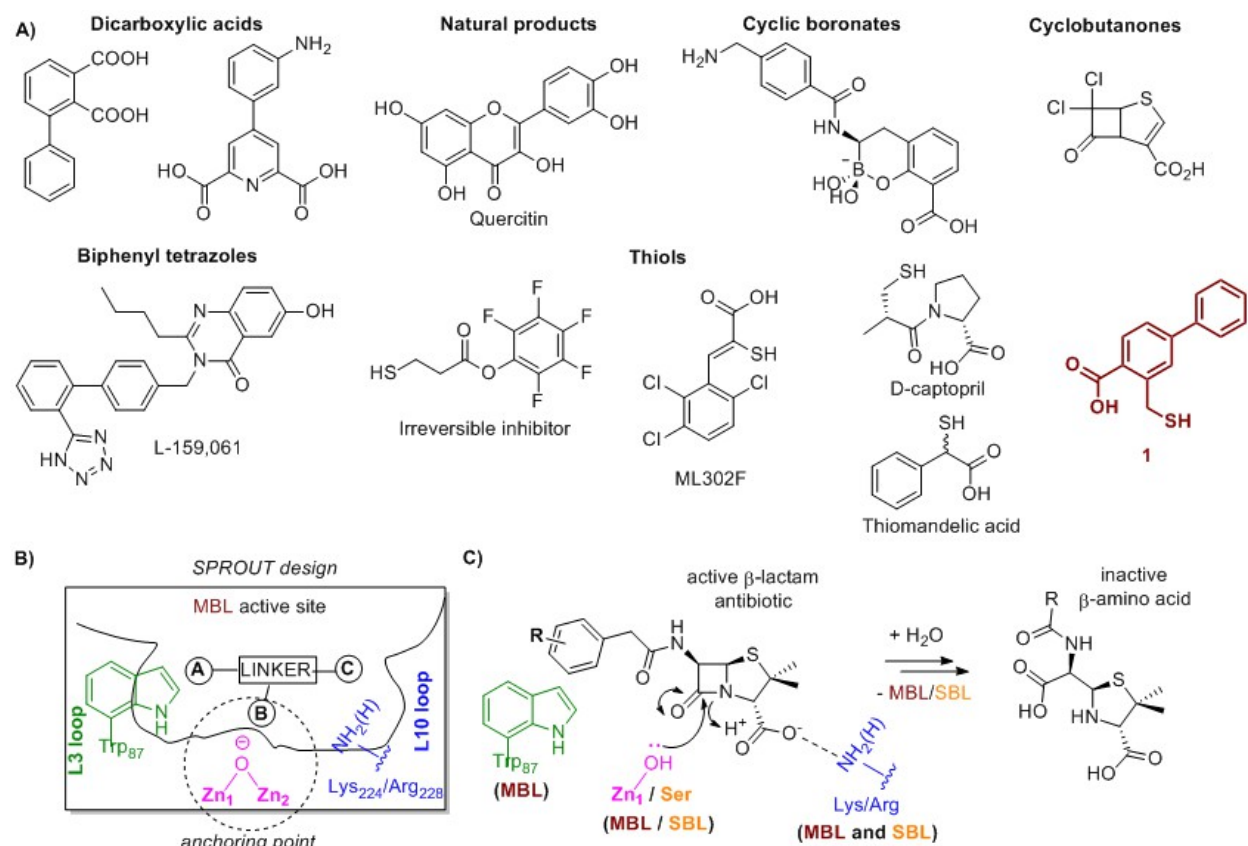


**Figure 2.** Predicted potential binding modes for the designed NDM-1 inhibitors and the crystallographically observed binding mode for VIM-2. (A), (C), and (D) shows views from modelling of **1** into the active sites of NDM-1, TEM-1, and OXA-10, respectively (see Supporting Information for details); (B) shows view from a crystal structure of **2** co-crystalized with VIM-2 (PDB ID: 5K48).

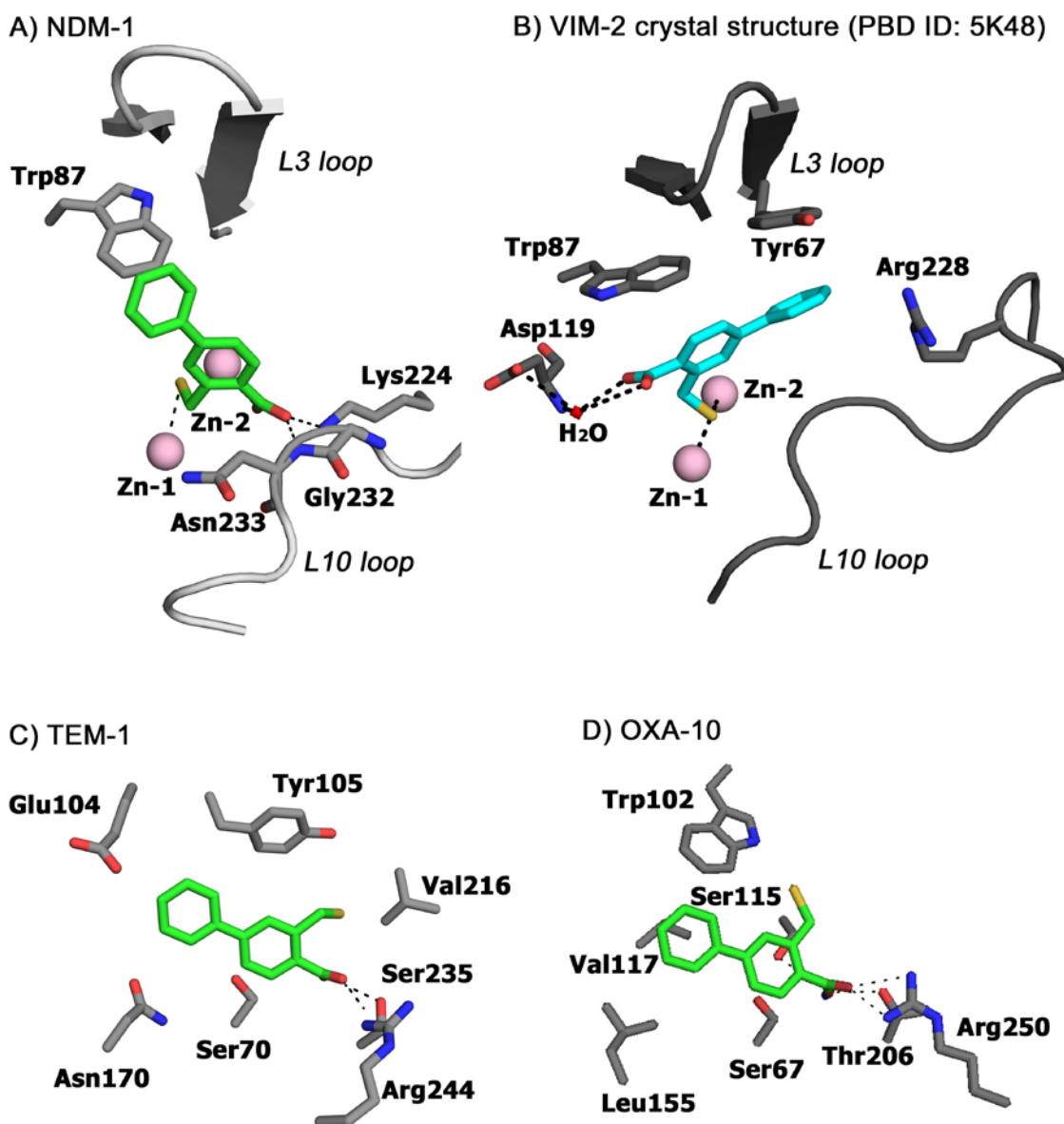
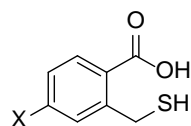


**Table 1.** IC<sub>50</sub> values of *de novo* designed thiols against clinically relevant B1 MBLs. Assays were conducted as reported<sup>20</sup>.



| No.       | X   | cLogP <sup>a</sup> | IC <sub>50</sub> NDM-1<br>(μM) | IC <sub>50</sub> VIM-2<br>(μM) | IC <sub>50</sub> IMP-1<br>(μM) |
|-----------|---|--------------------|--------------------------------|--------------------------------|--------------------------------|
| <b>1</b>  | C <sub>6</sub> H <sub>5</sub>                     | 3.76               | 5.59 ± 0.05                    | 0.23 ± 0.04                    | 0.23 ± 0.04                    |
| <b>4</b>  | 2-ClC <sub>6</sub> H <sub>4</sub>                 | 4.37               | 2.85 ± 0.03                    | 0.18 ± 0.09                    | 0.30 ± 0.06                    |
| <b>5</b>  | 3-ClC <sub>6</sub> H <sub>4</sub>                 | 4.37               | 0.31 ± 0.05                    | 0.07 ± 0.05                    | 0.14 ± 0.05                    |
| <b>6</b>  | 4-ClC <sub>6</sub> H <sub>4</sub>                 | 4.37               | 0.42 ± 0.02                    | 0.10 ± 0.03                    | 0.06 ± 0.05                    |
| <b>7</b>  | 3-FC <sub>6</sub> H <sub>4</sub>                  | 3.90               | 0.59 ± 0.02                    | 0.20 ± 0.06                    | 0.39 ± 0.08                    |
| <b>8</b>  | 4-FC <sub>6</sub> H <sub>4</sub>                  | 3.90               | 0.71 ± 0.01                    | 0.23 ± 0.03                    | 0.30 ± 0.09                    |
| <b>9</b>  | 2,3-ClC <sub>6</sub> H <sub>3</sub>               | 4.97               | 1.16 ± 0.05                    | 0.04 ± 0.03                    | 0.37 ± 0.06                    |
| <b>10</b> | 2-CF <sub>3</sub> C <sub>6</sub> H <sub>4</sub>   | 4.64               | 8.82 ± 0.05                    | 0.15 ± 0.08                    | 0.48 ± 0.04                    |
| <b>11</b> | 3,5-CF <sub>3</sub> C <sub>6</sub> H <sub>3</sub> | 5.52               | 43.95 ± 0.06                   | 0.45 ± 0.07                    | 1.72 ± 0.04                    |
| <b>12</b> | 2-Naphthyl  | 4.75               | 2.42 ± 0.03                    | 0.07 ± 0.03                    | 0.22 ± 0.03                    |
| <b>13</b> | 4-EtC <sub>6</sub> H <sub>4</sub>                 | 4.72               | 0.57 ± 0.02                    | 0.10 ± 0.03                    | 0.05 ± 0.03                    |
| <b>14</b> | 3-EtO-C <sub>6</sub> H <sub>4</sub>               | 3.96               | 7.59 ± 0.03                    | 0.18 ± 0.16                    | 0.32 ± 0.03                    |
| <b>15</b> | 2-Furyl   | 2.82               | 10.21 ± 0.04                   | 0.36 ± 0.02                    | 0.39 ± 0.03                    |
| <b>16</b> | 3-Thienyl   | 3.54               | 6.78 ± 0.09                    | 0.17 ± 0.12                    | 0.18 ± 0.04                    |
| <b>17</b> | Br  | 2.88               | > 100                          | 0.17 ± 0.01                    | 0.80 ± 0.03                    |

<sup>a</sup>cLogP values were calculated using MarvinSketch 17.28 (ChemAxon).

<sup>b</sup> The IC<sub>50</sub> values are shown as the mean ± SD from minimum three separate experiments.

**Table 2.** Determination of Meropenem MICs against bacterial strains when co-administered with the designed  $\beta$ -lactamase inhibitors. Assays were conducted as reported<sup>11</sup>.

| Compound<br>Number | X   | Meropenem MIC ( $\mu\text{g/mL}$ )<br>NDM-1 producing <i>K.</i><br><i>pneumoniae</i> (ATCC 5055) | Meropenem MIC ( $\mu\text{g/mL}$ )<br>NDM-1 producing <i>E. coli</i><br>(MG1655) |
|--------------------|---|--|--|
| Meropenem          |   | > 128  | > 128  |
| 1                  | C <sub>6</sub> H <sub>5</sub>                     | 32   | 16   |
| 17                 | Br  | 64   | 32   |
| 11                 | 3,5-CF <sub>3</sub> C <sub>6</sub> H <sub>3</sub> | >128   | >128   |
| 12                 | 2-Naphthyl  | 32   | 32   |
| 13                 | 4-Et-C <sub>6</sub> H <sub>4</sub>                | 64   | 32   |
| 14                 | 3-EtO-tC <sub>6</sub> H <sub>4</sub>              | 16   | 64   |
| 15                 | 2-Furyl   | 64   | 32   |
| 16                 | 3-Thienyl   | 8  | 16   |

## Table of Contents Graphic

